Inorg. Chem. **2008**, *47*, 4185−4198

Magnetic Circular Dichroism of Phthalocyanine (M = Mg, Zn) and Tetraazaporphyrin (M = Mg, Zn, Ni) Metal Complexes. A Computational Study Based on Time-Dependent Density Functional Theory

G. A. Peralta, Michael Seth, Hristina Zhekova, and Tom Ziegler*

Department of Chemistry, University of Calgary University Drive 2500, Calgary, Alberta, Canada

Received November 9, 2007

We present here simulated magnetic circular dichroism (MCD) spectra of MTAP (M = Mg, Ni, Zn) and MPc (M = Mg, Zn) where TAP = tetraazaporphyrin and *Pc* = phthalocyanine. The study is based on magnetically perturbed time-dependent density functional theory (MP-TDDFT) and a newly implemented method for the calculation of *A* and *B* terms from the theory of MCD. It follows from our investigation that the MCD spectrum for the MTAP and MPc systems in the *Q*-band region consists of a single positive *A* term augmented by a positive *B* term, in agreement with experiment where available. The *Q* band can be fully characterized in terms of the $2a_{1u} \rightarrow 2e_g$ one-electron excitation. For the aza systems MgTAP and ZnTAP, the simulated MCD spectra in the Soret region are dominated by the two one-electron excitations $2a_{2u} \rightarrow 2e_g$ and $1a_{2u} \rightarrow 2e_g$ and has the appearance of a positive *A* term (with values between 1.33−1.55, depending on the MTAP system) made asymmetric by a negative *B* term, in good agreement with experiment. We find, in agreement with all available experimental findings on MPc (M = Mg, Zn) type systems, that the MCD spectra in the Soret region are dominated by two transitions with positive *A*/*D*-term values and two negative *B*/*D*-term values. The major contribution to the two transitions comes from the $2a_{2u} \rightarrow 2e_g$ and $1a_{2u} \rightarrow 2e_g$ one-electron excitations. It appears that the ratio of *A*/*B* for the term parameters is underestimated by theory.

1. Introduction

We have in a recent study presented simulated magnetic circular dichroism (MCD) spectra[1] for simple metal porphyrins MgP, ZnP, NiP as well as MgTPP, ZnTPP, NiTPP (TPP = tetraphenylporphyrin), and NiOEP (OEP = octaethylporphyrin). The MCD simulations were based on a recent implementation[2] into the Amsterdam Density Functional program[3,4] based on time-dependent density functional theory (TD-DFT). Here, we report a theoretical study on the MCD spectra of phthalocyanine (M = Mg, Zn) and tetraazaporphyrin (M = Mg, Zn, Ni) metal complexes (Figure 1).

A molecule placed in a constant magnetic field will absorb right and left circular-polarized light differently as the light propagates through the molecule in the direction of the magnetic field. The difference in absorption is what is recorded in an MCD spectrum. In contrast to natural circular dichroism (CD) that is restricted to chiral molecules, induced magneto optical activity (MOA) can be observed for most molecules, and this fact makes the MCD methodology widely applicable. Thus, MCD has been applied to main-group molecules, transition-metal complexes, and biological systems.[5–7] The fundamental theory behind MCD has been worked out in great details[6,8–22] starting with the seminal

* To whom correspondence should be addressed. E-mail: Ziegler@ucalgary.ca.

(1) Peralta, G. A.; Seth, M.; Ziegler, T. *Inorg. Chem.* **2007**, *46*, 9111–9125.
(2) (a) Seth, M.; Ziegler, T.; Banerjee, A.; Autschbach, J.; van Gisbergen, S. J. A.; Baerends, E. J. *J. Chem. Phys.* **2004**, *120*, 10942–10954. (b) Seth, M.; Autschbach, J.; Ziegler, T. *J. Chem. Phys.* **2005**, *122*−1−7. (c) Seth, M.; Ziegler, T. *J. Chem. Phys.* **2006**, *124*−1−12. (d) Seth, M.; Autschbach, J.; Ziegler, T. *J. Chem. Theory Comput.* **2007**, *3*, 434–447. (e) Krykunov, M.; Banerjee, A.; Ziegler, T.; Autschbach, J. *J. Chem. Phys.* **2005**, *122*, 075105.
(3) Baerends, E. J.; Ellis, D. E.; Ros, P. *Chem. Phys.* **1973**, *2*, 41–51.
(4) (a) te Velde, G.; Baerends, E. J. *J. Comput. Phys.* **1992**, *99*, 84–98. (b) Fonseca Guerra, C.; Visser, O.; Snijders, J. G.; te Velde, G.; Baerends, E. J. Parallelisation of the Amsterdam Density Functional Program. In *Methods and Techniques for Computational Chemistry*; Clementi, E. Corongiu, G. Eds.; STEF: Cagliari, 1995; pp. 305−395.
(5) (a) *The Porphyrins, Vol, III, Part A*; Dolphin, D. Ed.; Academic Press: New York, 1978−1979. (b) *Porphyrins and Metalloporphyrins*; Smith K. M., Ed.; Elsevier Scientific Publishing Company: Amsterdam, 1975.
(6) Solomon, E. I.; Brunold, T.; Davis, M. I.; Kemsley, J. N.; Lee, S.-K.; Lehnert, N.; Nesse, F.; Skulan, A. J.; Shan, Y.-S.; Zhou, J. *Chem. Rev.* **2000**, *100*, 235–350.

10.1021/ic7022117 CCC: $40.75
Published on Web 04/23/2008

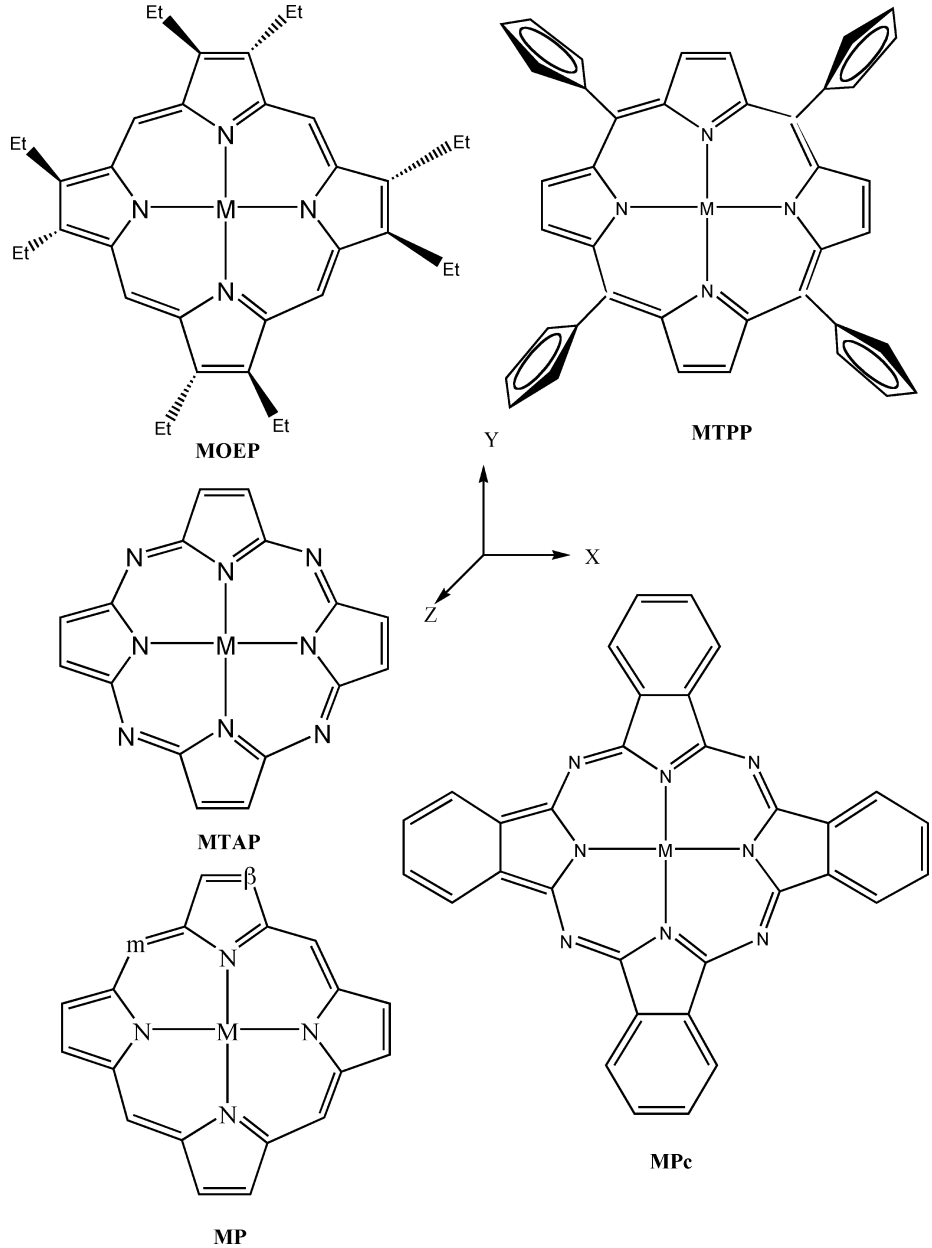

Figure 1. Different porphyrin complexes mentioned in this study. Normal porphyrin (MP), tetraazaporphyrin (MTAP), tetraphenylporphyrin (MTPP), octaethylporphyrin (MOEP), and phthalocyanine (MPc).

work by Stephens[10] and Buckingham. The subject has further been discussed in two text books,[19,22] and several recent reviews have covered the application of MCD to porphyrin and phthalocyanine complexes.[23–25] There are numerous computational studies on the electronic structure and ultraviolet adsorption spectrum of phthalocyanine, tetraazaporphyrin, and porphyrin complexes based on semiempirical, DFT, and ab initio methods.[23–33] On the other hand, computational studies involving the direct calculation of *A* and *B* terms from the theory of MCD are rare and have until recently been limited to semiempirical methods[31–33] aside

(7) *Expanded Contracted and Isomeric Porphyrins*, Vol. *15*; Baldwin, J. E., Magnus, P. D., Eds.; Pergamon, 1997.
(8) Prasad, D. R.; Ferraudi, G. *Inorg. Chem.* **1983**, *22*, 1672–1674.
(9) VanCott, T. C.; Rose, J. L.; Misener, G. C.; Williamson, B. E.; Schrimpf, A. E.; Boyle, M. E.; Schatz, P. N. *J. Chem. Phys.* **1989**, *93*, 2999.
(10) (a) Stephens, P. J. *Annu. Rev. Phys. Chem.* **1974**, *25*, 201. (b) Stephens, P. J. *Adv. Chem. Phys.* **1976**, *35*, 197–264. (c) Buckingham, A. D.; Stephens, P. J. *Annu. Rev. Phys. Chem.* **1966**, *17*, 399.
(11) Michl, J. *J. Am. Chem. Soc.* **1978**, *100*, 6801–6824.
(12) Ballhausen, C. J. *Molecular Electronic Structure of Transition Metal Complexes*; McGraw-Hill: New York, 1979.
(13) Darwent, J. R.; Douglas, P.; Harriman, A.; Porter, G.; Richoux, M. C. *Coord. Chem. Rev.* **1982**, *44*, 83–126.
(14) Lever, A. B. P.; Licoccia, S.; Ramaswamy, B. S.; Kandil, S. A; Stynes, D. V. *Inorg. Chim. Acta* **1981**, *51*, 163–167.
(15) Ohtani, H.; Kobayashi, T.; Ohno, T.; Kato, S.; Tanno, T.; Yamada, A. *J. Phys. Chem.* **1984**, *88*, 4431–4435.
(16) Kobayashi, T.; Nishiyama, T. *J. Phys. Chem.* **1985**, *89*, 1167–1170.
(17) Van Den Brink, F.; Visscher, W.; Barendrecht, E. *J. Electroanal. Chem. Interfacial Electrochem.* **1985**, *175*, 279–289.
(18) Ferraudi, G.; Prasad, D. R. *J. Chem. Soc., Dalton Trans.* **1984**, 2137–2140.
(19) (a) Piepho, S. B.; Schatz, P. N. *Group Theory in Spectroscopy with Applications to Magnetic Circular Dichroism*; Wiley: New York, 1983. (b) Equation A.4.13 of Ref. 19a. (c) Equation A.4.10 of ref 19a. (d) Equation 4.6.14 of ref 19a.
(20) Prasad, D. R.; Ferraudi, G. *J. Phys. Chem.* **1984**, *88*, 4037–4040.

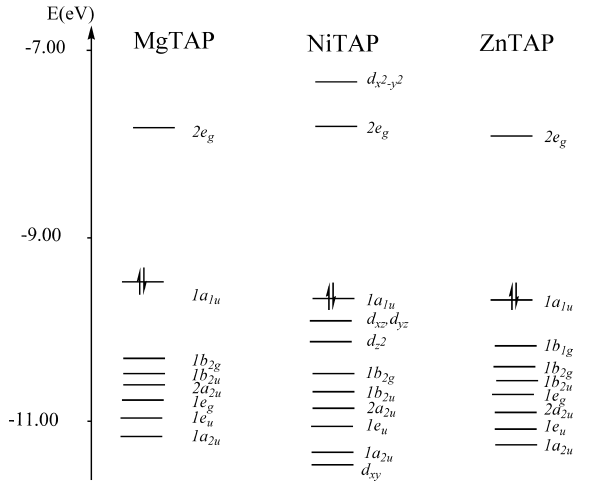

Figure 2. Molecular orbital energy level diagram for MTAP.

from the DFT based investigation[1] on porphyrins published in 2007 by our group. The present study represents the first ab initio investigation of *A* and *B* terms for phthalocyanine (M = Mg, Zn) and tetraazaporphyrin (M = Mg, Zn, Ni) metal complexes. As we shall see, the MCD spectrum of the title compounds differs considerably from that of porphyrins as far as electronic origin, intensity, and relative importance of *A* and *B* terms are concerned.

Porphyrins are often used to model chlorophylls and heme proteins,[5–13,34] and they have been found to be essential for a number of physiological and biological functions such as respiration and photosynthesis. In addition, porphyrins are used in many practical applications including dyes and pigments. Their optical properties have further shown great potential in technological applications such as linear and nonlinear optics,[35–44] photodynamic therapy,[45,46] electroop-

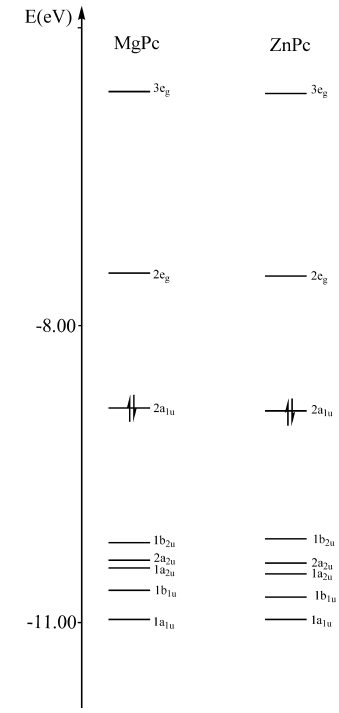

Figure 3. Molecular orbital energy level diagram for MPc.

tics,[40–46] photonics,[40–44] and catalysis.[47,48] It is common for all of the usages of porphyrins and their derivatives in nature, that an understanding for the way they function requires insight into their electronic structure, and such an insight is also required for the development of new technological applications of porphyrins.

This account is organized as follows. The section on Computational Methods and Details introduces the fundamental aspects of MCD. The section on Computational Methods and Details begins with a discussion of the molecular orbital level diagrams for phthalocyanine (M = Mg, Zn) and tetraazaporphyrin (M = Mg, Zn, Ni) metal complexes in conjunction with their recorded absorption UV spectrum. The second part of Results and Discussion introduces our simulated MCD spectra for MPc (M = Mg, Zn) and MTAP (M = Mg, Zn, Ni) and compares them to experimental results as well as our previously simulated MCD spectra[1] for the simple porphyrins MgP, ZnP, NiP as well as MgTPP, ZnTPP, NiTPP (TPP = tetraphenylporphy-

(21) Ohno, T.; Kato, S. *J. Phys. Chem.* **1984**, *88*, 1670–1674.
(22) Mason. W. R. *A Practical Guide to Magnetic Circular Dichroism Spectroscopy*; Wiley, 2007.
(23) Mack, J.; Stillman, M. *J. Inorg. Chem.* **1997**, *36*, 413–425.
(24) (a) Mack, J.; Stillman, M. J. *J. Porphyrins Phthalocyanines* **2001**, *5*, 67–76. (b) Mack, J.; Stillman, M. J.; Kobayashi, N. *Coord. Chem. Rev.* **2007**, *251*, 429–453. (c) Kobayashi, N.; Nakai, K. *Chem. Commun.* **2007**, *40*, 4077–4092.
(25) (a) Kobayashi, N.; Mack, J.; Ishii, K.; Stillman, M. *J. Inorg. Chem.* **2002**, *41*, 5350–5363. (b) Mack, J.; Asano, Y.; Kobayashi, N.; Stillman, M. J. *J. Am. Chem. Soc.* **2005**, *127*, 17697–17711.
(26) Henriksson, A.; Sundbom, M. *Theoret. Chim. Acta* **1972**, *27*, 213–222.
(27) Edwards, L.; Gouterman, M. *J. Mol. Spectrosc.* **1970**, *33*, 292–310.
(28) Zhou, X.; Ren, A.; Feng, J.; Liu, X. *Can. J. Chem.* **2004**, *82*, 19–26.
(29) Cory, M. G.; Hirose, H.; Zerner, M. C. *Inorg. Chem.* **1995**, *34*, 2969–2979.
(30) Baerends, E. J.; Ricciardi, G.; Rosa, A.; van Gisbergen, S. J. A. *Coord. Chem. Rev.* **2002**, *230*, 5–27.
(31) Kaito, A.; Nozawa, T.; Yamamoto, T.; Hatano, M. *Chem. Phys. Lett.* **1977**, *52*, 154–160.
(32) Mack, J.; Stillman, M. J. *J. Phys. Chem.* **1995**, *99*, 7935–7945.
(33) Mack, J.; Stillman, M. J. *Coord. Chem. Rev.* **2001**, *993*, 219–221.
(34) Dolphin, D.; James, B. R.; Murray, A. J.; Thornback, J. R. Can. *J. Chem.* **1980**, *58*, 1125–1132.
(35) Mansour, K.; Alverex, D., Jr.; Perry, K. J.; Choong, I.; Marder, S. R.; Perry, J. W. *Proc. SPIE.* **1993**, *1853*, 132–142.
(36) Su, W.; Cooper, T. M.; Brant, M. C. *Chem. Mater.* **1998**, *10*, 1212–1213.
(37) Qureshi, F. M.; Martin, S. J.; Long, X.; Bradley, D. D. C.; Henari, F. Z.; Blau, W. J.; Smith, E. C.; Wang, C. H.; Kar, A. K.; Anderson, H. L. *Chem. Phys.* **1998**, *231*, 87–94.
(38) Stiel, H.; Volkmer, A.; Ruckmann, I.; Zeug, A.; Ehrenberg, B.; Roder, B. *Opt. Commun.* **1998**, *155*, 135–137.
(39) de la Torre, G.; Vazquez, P.; Agullo-Lopez, F.; Torres, T. *J. Mater. Chem.* **1998**, *8*, 1671–1683.
(40) Pryadarshy, S.; Therien, M. J.; Beratan, D. N. *J. Am. Chem. Soc.* **1996**, *118*, 1504–1510.
(41) Beljonne, D.; O'Keefe, G. E.; Hamer, P. J.; Friend, R. H.; Anderson, H. L.; Brédas, J. L. *J. Chem. Phys.* **1997**, *106*, 9439–4960.
(42) Henari, F. Z.; Blau, W. J.; Milgrom, L. R.; Yahioglu, G.; Phillips, D.; Lacey, J. A. *Chem. Phys. Lett.* **1997**, *267*, 229–233.
(43) Wang, Z.; Day, P. N.; Pachter, R. *J. Chem. Phys.* **1998**, *108*, 2504–2510.
(44) Chen, P.; Tomov, I. V.; Dvornikov, A. S.; Nakashima, M.; Roach, J. F.; Alabram, D. M.; Rentzepis, P. M. *J. Phys. Chem.* **1996**, *100*, 17507–17512.
(45) Bonnett, R. *Chem. Soc. Rev.* **1995**, *24*, 19–33.
(46) Rosenthal, I.; Ben-Hur, E. In *Phthalocyanines*; Leznoff, C. C., Lever, A. B. P., Eds.; VCH: New York, 1989; p 393.
(47) Moser, F. H.; Thomas, A. L. *The Phthalocyanines*; CRC: Boca Raton, FL, 1983.
(48) Seto, J.; Tamura, S.; Asai, N.; Kishii, N.; Kijima, Y.; Matsuzawa, N. *Pure Appl. Chem.* **1996**, *68*, 1429–1434.

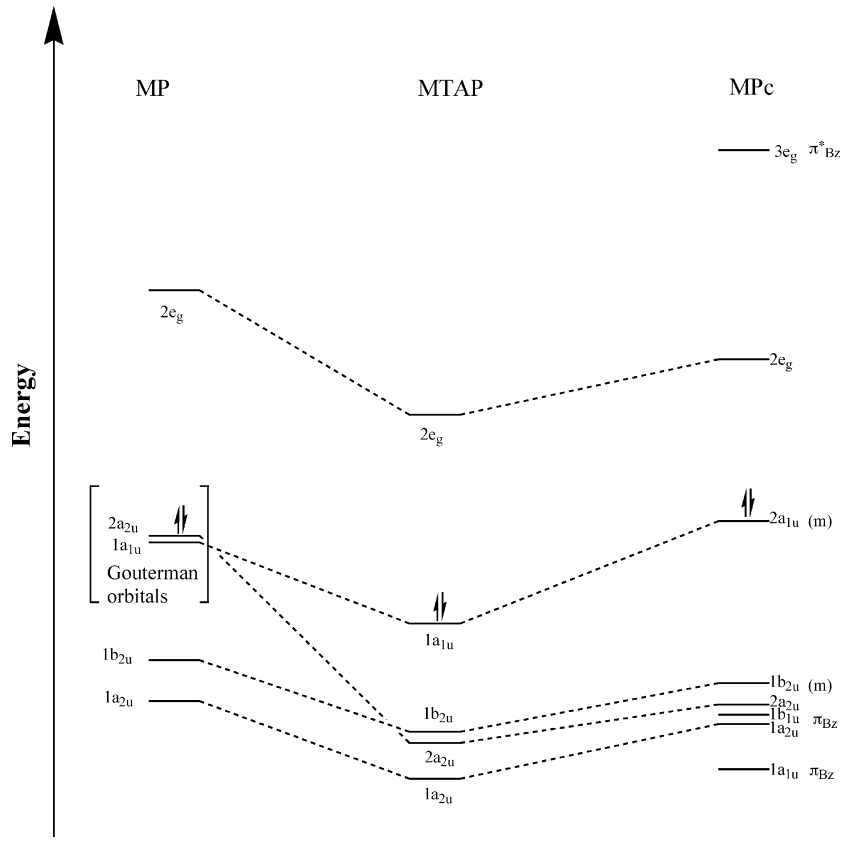

Figure 4. Comparison of molecular orbital energy levels for MP, MTAP, and MPc. The actual orbital energies are from ZnL (L = P, TAP, Pc).

rin) and NiOEP (OEP = octaethylporphyrin). We finally comment on how our findings compare to previously published assignments of the *Q* and Soret bands[49–55] The reader is referred to a recent review on the application of MCD spectroscopy to porphyrinoids.[24b] The application of theoretical methods to the electronic structure and UV spectra of these species has also been review recently.[30]

2. Theoretical Method and Computational Details

2.1. Details of the Calculations. In this study, use was made of the Amsterdam program package ADF and its implementation of the time-dependent density functional theory.[56–59] The BP86 functional due to Becke[60] and Perdew[61] was employed for structure optimization. On the other hand, the SAOP potential (Statistical averaging of different orbital-dependent model potentials)[62,63] was adopted for all TD-DFT-based simulations of UV and MCD spectra. UV absorption spectra of metal NiP, NiPc, and NiTAP complexes have in the past[1,12,64] been modeled successfully by the SAOP potential.

The electric dipole and spin-allowed transitions in the title compounds are from the singlet $^1A_{1g}$ ground state to the singlet $^1A_{2u}$ and ^1E_u excited states. All of these transitions have been calculated in the range of 2−6 eV. Because only singlet transitions are considered here, we shall in the following omit the superscript indicating the spin multiplicities for the sake of brevity. Use was made of the frozen-core approximation in optimizing the ground-state structures.. The core was defined as $1s^2$ of carbon and nitrogen, $1s^22s^22p^6$ of magnesium, and $1s^22s^22p^63s^23p^6$ of nickel and zinc. The basis consisted of a set of triple-ζ STO valence functions for all of the elements. The valence set was augmented by a set of single-ζ STO polarization functions as follows: 2p and 3d for hydrogen; 3d and 4f for carbon and nitrogen; 3p, 3d, and 4f for magnesium; 4s, 4p, and 4f for nickel; and 4p and 4f for zinc. The structures for the title compounds were all optimized under a D_{4h} symmetry constraint for all of the

(49) Gouterman, M. *J. Chem. Phys.* **1959**, *30*, 1139–1151.
(50) Gouterman, M. *J. Mol. Spectrosc.* **1961**, *6*, 138–163.
(51) Gouterman, M.; Wagnière, G.; Snyder, L. C. *J. Mol. Spectrosc.* **1963**, *11*, 108–127.
(52) Gouterman, M. *J. Mol. Spectrosc.* **1972**, *44*, 37–80.
(53) Schaffer, A. M.; Gouterman, M.; Weiss, C. *Theor. Chim. Acta* **1973**, *30*, 9–30.
(54) Weiss, C., Jr.; Kobayashi, H.; Gouterman, M. *J. Mol. Spectrosc.* **1965**, *16*, 415–450.
(55) McHugh, A. J.; Gouterman, M.; Weiss, C., Jr. *Theor. Chim. Acta* **1972**, *24*, 346–370.
(56) Casida, M. E. In *Recent Advances in Density Functional Methods;* Chong, D. P., Ed.; World Scientific: Singapore, Vol. *1*, 1995; p 155.
(57) Gross, E. K. U.; Kohn, W. *Adv. Quantum Chem.* **1990**, *21*, 255–291.
(58) Gross, E. K. U.; Ullrich, C. A. Gossmann, U. J. *Density Functional Theory of Time-Dependent Systems*; Plenum: New York, Vol. *337* of NATO ASI Ser. B., 1995; p 149M.
(59) Gross, E. U. K.; Dobson, J. F.; Petersilka, M. Density Functional Theory. In *Springer Series: Topics in Current Chemistry*; Nalewajski, R. F., Ed.; Springer: Heidelberg, Germany, 1996.
(60) Becke, A. *Phys. Rev.* **1988**, *38*, 3098–3100.
(61) Perdew, J. P. *Phys. Rev.* **1986**, *33*, 8822–8824, Erratum: PRB 347406), 1986.
(62) Gritsenko, O. V.; Schipper, P. R. T.; Baerends, E. *J. Chem. Phys. Lett.* **1999**, *302*, 199–207.
(63) Schipper, P. R. T.; Gritsenko, O. V.; van Gisbergen, S. J. A.; Baerends, E. J. *J. Chem. Phys.* **2000**, *112*, 1344–1352.
(64) Rosa, A.; Ricciardi, G.; Baerends, E. J.; van Gisbergen, S. J. A. *J. Phys. Chem. A* **2001**, *105*, 3311–3327.

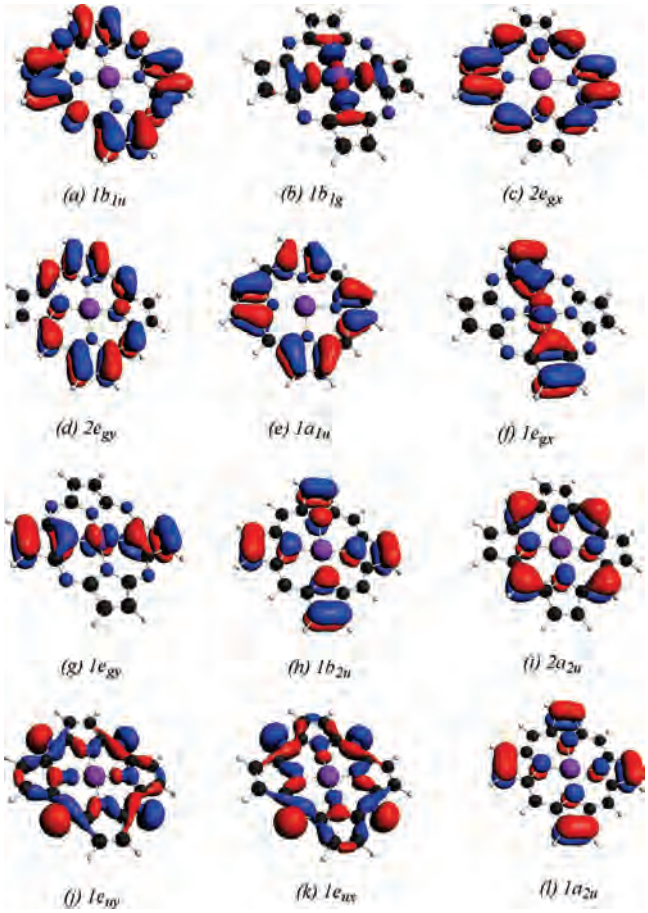

Figure 5. Key orbitals for MTAP.

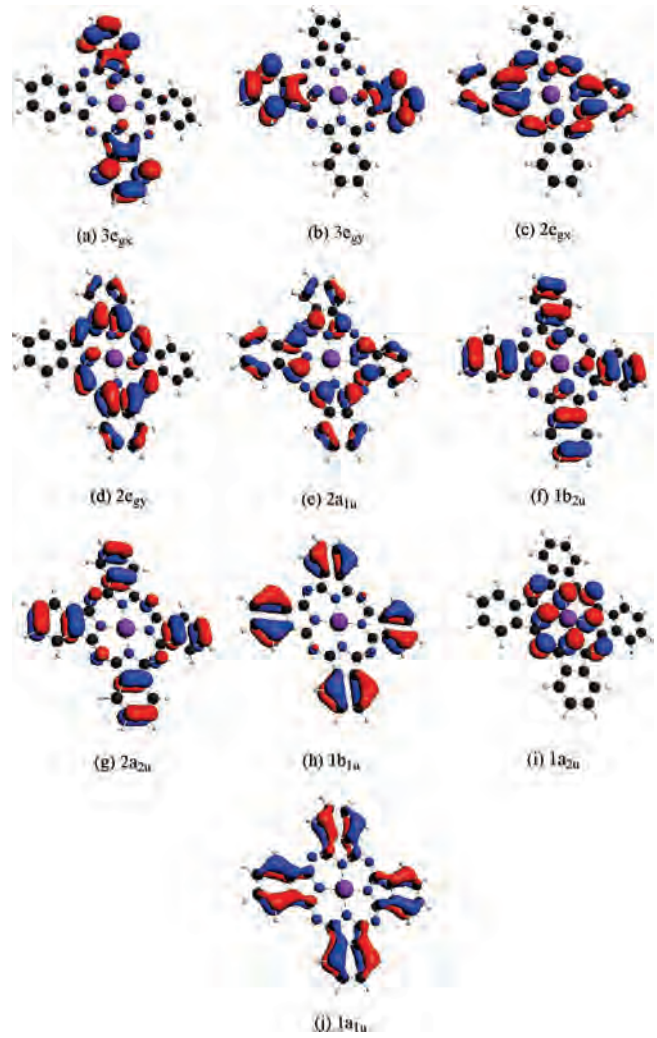

Figure 6. Key orbitals for MPc.

studied molecules. The routines used to calculate the angular momentum integrals required in this study were introduced in connection with the implementation of a method for the calculation of the Verdet constant.[2e] As in the previous study on porphyrins,[1] vibronic coupling is completely neglected.

2.2. Magnetic Circular Dichroism. When a molecule is placed in a constant magnetic field with strength B, it will absorb right and left circular-polarized light differently as the light propagates through the molecule in the direction of the magnetic field. In MCD this difference can be expressed in terms of the molar extinction coefficient[19] ε of left ($\varepsilon_-(\omega)$) and right ($\varepsilon_+(\omega)$) circular polarized light after averaging over the orientation of the molecules in the sample relative to the direction of the magnetic field given as, [19b]

$$\varepsilon_-(\omega) - \varepsilon_+(\omega) = \Delta\varepsilon = \lambda_o \mu_B \hbar\omega \left(\sum_J -A_{AJ} \frac{\partial \rho_{AJ}(\omega)}{\partial \omega} + \left(B_{AJ} + \frac{C_{AJ}}{kT} \right) \rho_{AJ}(\omega) \right) B \quad (1)$$

where:[19c]

$$\lambda_0 = \frac{2N_0 \pi^3 \vartheta^2 (c'\, l) \log e}{250 hcn} \quad (2)$$

In eq 2, the proportionality constant ϑ relates the macroscopic electric field of the incident light with the corresponding microscopic field experienced by the molecule, $\rho_{AJ}(\omega)$ is the density of states function for the transition from the ground state (A) to an excited state (J) as a function of the angular frequency of light ω. In addition, h is the Planck constant, c is the speed of light, n is the refractive index, N_0 is Avogadro's number, and μ is the Bohr magneton. Finally, c′ is the concentration of the sample in solution and l is the path length through the solution containing the sample. We shall in our simulations represent $\rho_{AJ}(\omega)$ with a Gaussian band shape function $f_J(122)$ given by

$$f_J(\omega) = \frac{1}{\Omega_J \sqrt{\pi}} \exp[-(\hbar\omega - \hbar\omega_J)^2 / \Omega_J^2] \quad (3)$$

where $W_J = \hbar\omega_J$ is the energy of the excited-state J relative to the ground-state A. Further, ΩJ is a bandwidth parameter taken from experimental spectra. A useful empirical relation is $\Omega J = 0.08 \times \sqrt{W_J}$ with W_J in eV.

The A-term parameter A_{AJ} in eq 1 represents a contribution to $\Delta\varepsilon(\omega)$ for systems that have degeneracies in the ground-state, the excited state, or in both. The magnetic field can split the degenerate states in such a way that it leads to a difference in the absorption of left- and right-polarized light[19] at the absorption frequency. The B_{AJ} term parameter in eq 1 represents the contribution to $\Delta\varepsilon(\omega)$ from the mixing of the A with all other excited states K due to the external homogeneous magnetic field $\vec{\mathbf{B}}$, as well as the mixing induced by $\vec{\mathbf{B}}$ between J and all other excited states K. The

Table 1. Calculated Excitation Energies (eV), Oscillator Strength (*f*), and A^b, *A*/*D*, B^b and *B*/*D* parameters for MTAP (M = Mg, Ni, Zn)

		excitation energies									
complex	symmetry	exptl	calcd	composition	%	*f*	*A*	*A*/*D*	*B*	*B*/*D*	assign.
MgTAP	$1E_u$		2.32	$1a_{1u} \rightarrow 2e_g$	74.82	0.474	6.86	4.94	172.49	124.09	*Q*
				$2a_{2u} \rightarrow 2e_g$	20.89						
	$2E_u$		2.79	$1b_{2u} \rightarrow 2e_g$	97.27	0.048	−0.31	−2.64	43.10	369.51	
	$1A_{2u}$		3.04	$1e_u \rightarrow 2e_g$	99.02	0.001	0.00	0.00	3.73	657.25	
	$3E_u$		3.08	$1a_{2u} \rightarrow 2e_g$	61.32	0.088	0.55	2.87	88.95	461.35	B_1
				$2a_{2u} \rightarrow 2e_g$	34.07						
				$2a_{2u} \rightarrow 2e_g$	42.25						
	$4E_u$		3.70	$1a_{2u} \rightarrow 2e_g$	31.79	3.280	1.33	0.22	−341.82	−56.68	B_2
				$1a_{1u} \rightarrow 2e_g$	1.84						
NiTAP	$1E_u$		2.39	$1a_{1u} \rightarrow 2e_g$	83.58	0.522	6.76	4.56	193.27	130.25	*Q*
				$2a_{2u} \rightarrow 2e_g$	13.78						
	$2E_u$		2.98	$1b_{2u} \rightarrow 2e_g$	97.11	0.046	−0.27	−2.59	19.55	190.06	
	$1A_{2u}$		3.29	$1e_u \rightarrow 2e_g$	98.76	0.001	0.00	0.00	3.33	809.44	
	$3E_u$		3.34	$1a_{2u} \rightarrow 2e_g$	84.67	0.004	0.02	2.27	−3.87	−545.85	
				$1e_g \rightarrow 1b_{1u}$	12.74						
	$2A_{2u}$		3.44	$1b_{2u} \rightarrow 1b_{1g}$	99.84	0.000	0.00	0.00	−0.12	−127.73	
	$4E_u$		3.47	$1e_g \rightarrow 1b_{1u}$	52.35	0.230	0.12	0.27	−227.53	−505.26	B_1
				$2a_{2u} \rightarrow 2e_g$	35.58						
				$1e_u \rightarrow 1b_{1g}$	42.18						
	$5E_u$		3.69	$1e_g \rightarrow 1b_{1u}$	25.55	0.574	−0.58	−0.55	−181.42	−171.24	B_2
				$2a_{2u} \rightarrow 2e_g$	17.54						
				$1a_{2u} \rightarrow 2e_g$	8.65						
ZnTAP	$1E_u$	1.95[a]	2.35	$1a_{1u} \rightarrow 2e_g$	77.68	0.258	7.29	4.89	201.55	135.34	*Q*
				$2a_{2u} \rightarrow 2e_g$	18.75						
	$2E_u$		2.83	$1b_{2u} \rightarrow 2e_g$	97.33	0.024	−0.30	−2.64	40.00	349.20	
	$1A_{2u}$		3.10	$1e_u \rightarrow 2e_g$	98.93	0.001	0.00	0.00	3.40	743.49	
	$3E_u$		3.16	$1a_{2u} \rightarrow 2e_g$	73.81	0.015	0.18	2.83	42.60	671.11	B_1
				$2a_{2u} \rightarrow 2e_g$	23.09						
				$2a_{2u} \rightarrow 2e_g$	54.59						
	$4E_u$	3.24[a]	3.69	$1a_{2u} \rightarrow 2e_g$	20.14	1.446	1.55	0.29	−314.96	−59.11	B_2
				$1a_{1u} \rightarrow 2e_g$	17.05						

[a] Experimental data from ref 67 correspond to a derivative (ZnTAPOP) of ZnTAP with phenyl groups at the b-positions. [b] Atomic units.

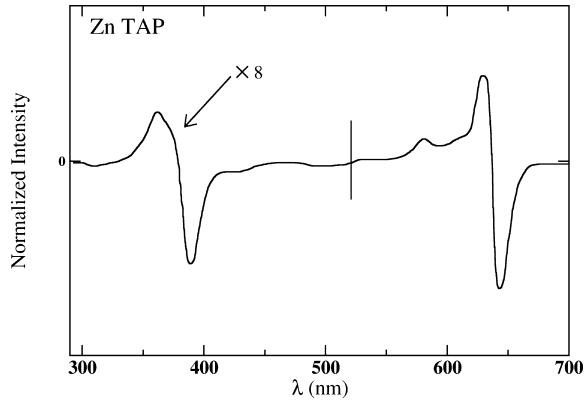

Figure 7. Experimental[67] MCD spectrum for ZnTAP. The actual compound (ZnTAPOP) has phenyl groups rather than hydrogens (ZnTAP) in the b-positions.

last parameter C_{AJ} in eq 1 is of importance for systems with degenerate a ground state where the population of the different components α in the presence of $\mathbf{B}^{\rightarrow}$ might differ as a function of *T*. The variation in the population with *T* will give a temperature-dependent contribution to $\Delta\varepsilon(\omega)$. This *C* term will not be of importance in the present study involving porphyrins with a closed-shell ground state and is not discussed any further here.[19] The expressions for *A*, *B*, and *C* are given elsewhere.[19,1] We refer to the literature for the way in which time-dependent density functional theory (TD-DFT)[65,66] is used to evaluate the *A*,[2a] *B*,[2d] *C*[2b,c] terms as well as the dipole strength *D*.[56]

3. Results and Discussion

It is useful to start our presentation of the simulated MCD spectra for the tetraazaporphyrin (TAP) and phthalocyanine (*Pc*) metal complexes by briefly reviewing the orbital levels and absorption spectra of these systems. A much more comprehensive theoretical account of the same subject can be found in a recent review by by Baerends[30] et al. The orbital levels for the MTAP and MPc systems are displayed in Figures 2 and 3, respectively. Please note that we only count the upper valence orbitals, starting with those of lowest energy.

3.1. Orbital Levels in MTAP and MPc. The two types of complexes (MTAP and MPc) studied here were considered to have D_{4h} symmetry, in line with previous experimental and theoretical works[20,30] (Figure 1). All of the complexes were placed in the *XY* plane with the C_4 axis pointing in the *z* direction and the *x*, *y* axes along the M−N bond vectors (Figure 1).

Our calculations indicate that the lowest unoccupied ligand-based levels in the MTAP and MPc systems are 2-fold degenerate and represented by a set of π^* orbitals of e_g symmetry, in agreement with previous theoretical studies cited in a recent review[30] (Figures 2 and 3). Also, in accordance with previous calculations,[30] we found in our study on MP[1] that the two occupied levels of highest energy

(65) Bauernschmitt, R.; Ahlrichs, R. *Chem. Phys. Lett.* **1996**, *256*, 454–464.
(66) van Gisbergen, S. J. A. Ph.D. Thesis, Vrije University, Amsterdam, The Netherlands, 1999.

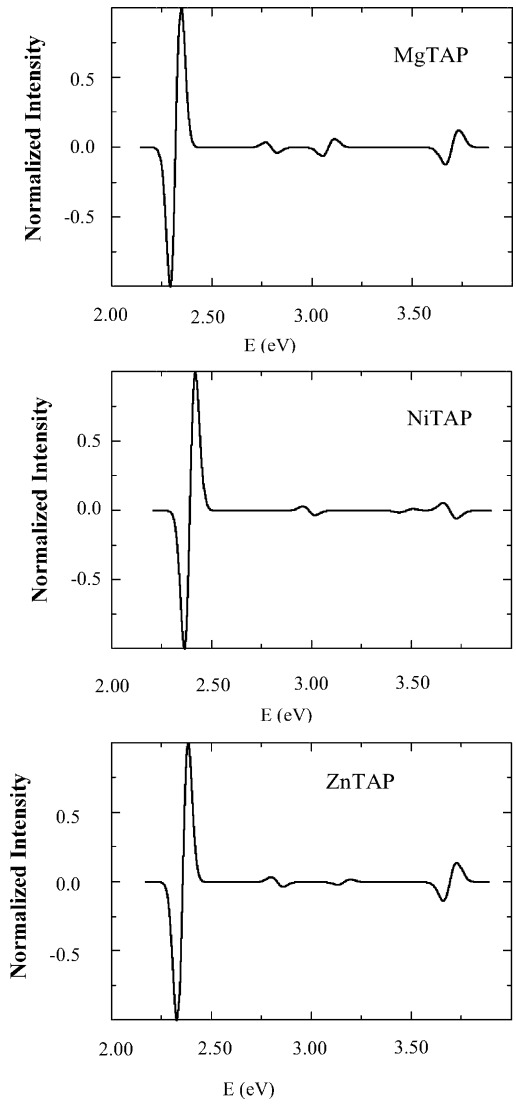

Figure 8. Simulated MCD spectra of MTAP based on *A* terms alone with M = Mg, Ni, Zn.

Table 2. Some of the Relevant Integrals Used to Calculate the *A*/*D* term for the *Q* and *B* bands of MTAP

	Zn	Mg	Ni
$\mathrm{Im}\langle 2e_{gx}\lvert\hat{l}_z\rvert 2e_{gy}\rangle$	−2.7287	−2.7486	−2.6325
$\mathrm{Im}\langle 1a_{1u}\lvert\hat{l}_z\rvert 2a_{2u}\rangle$	2.2430	2.0528	2.6023

were nearly degenerate and represented by π^* orbitals of a_{2u} and a_{1u} symmetry (Figure 4). The $2a_{2u}$ orbital of the regular porphyrins (MP, MTPP, and MOEP) has a large contribution from the π orbital of the carbon atom in the *m* position, whereas no such contribution[64] is present in $1a_{1u}$. Here, the *m* position is indicated for MP in Figure 1. As the carbon atom in MP now is substituted by the more electronegative nitrogen in MTAP and MPc, the energy of $2a_{2u}$ is lower compared to that of $1a_{1u}$, where the composition is unchanged (Figure 4). As pointed out by Baerends[30,64] et al., the change in the relative energies of $1a_{1u}$ and $2a_{2u}$ will make the composition of the excited states in MP, MTPP, MOEP quite different from those in MTAP and MPc. The shape of the key orbitals in MTAP and MPc are given in Figures 5 and 6, respectively.

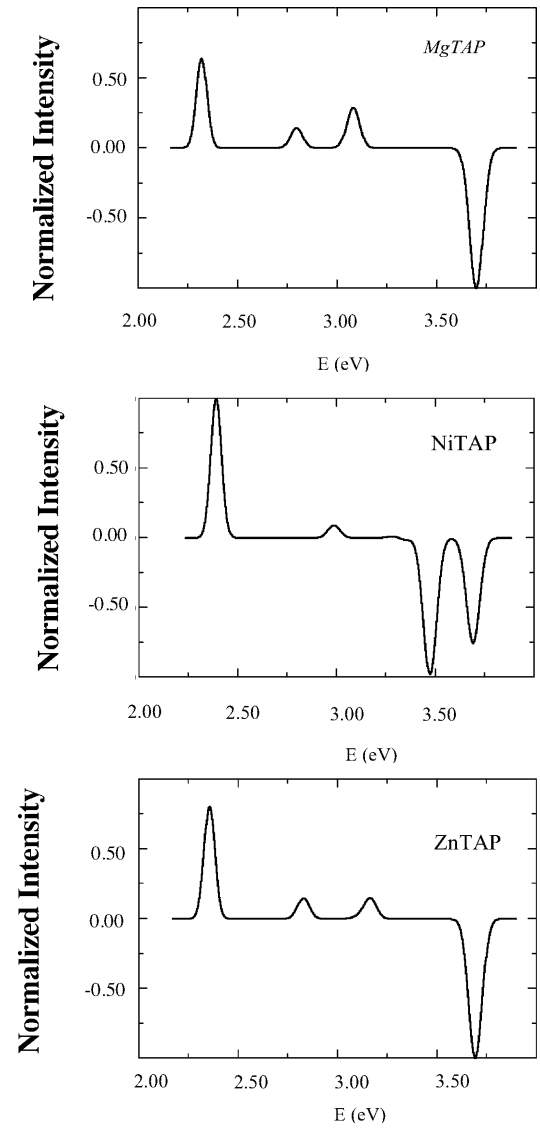

Figure 9. Simulated MCD including only the *B* terms due to the mixing of different excited states for the MTAP systems.

Our calculations seem to indicate that the valence-based orbitals for the MTAP and MPc systems are quire similar in terms of energy and symmetry for both the higher occupied or lower unoccupied orbitals irrespective of the metal (Figures 2 and 3). It is thus clear that the metal center has only a minor influence on these orbitals. Nevertheless, complexes containing a nickel center have an energy-level diagram that differs somewhat from the rest of the studied systems for the same ligand. These differences are a consequence of the empty-valence d orbital located below the lowest empty ligand orbital and four occupied d orbitals situated among the highest occupied π^* ligand levels (Figure 2 for NiTAP). The empty d-based orbital of b_{1g} symmetry has a 61% contribution from $d_{x^2-y^2}$, whereas the highest occupied d orbitals are the doubly degenerate level of e_g symmetry represented by two orbitals that have a contribution of 63% from d_{yz} and d_{xz}, respectively. The next level of a_{1g} symmetry has a contribution of 86% from d_{z^2}, whereas the lowest d level belonging to the b_{2g} representation has a 90% contribution from the d_{xy} orbital. Of the three d_π orbitals, d_{xy}

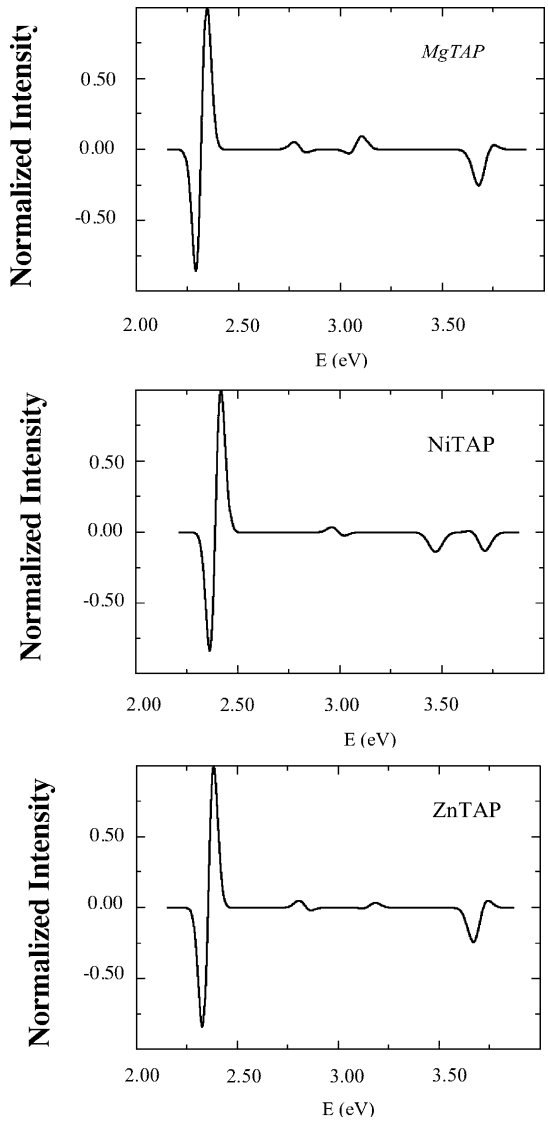

Figure 10. Simulated MCD spectra including both *A* and *B* terms for the MTAP systems.

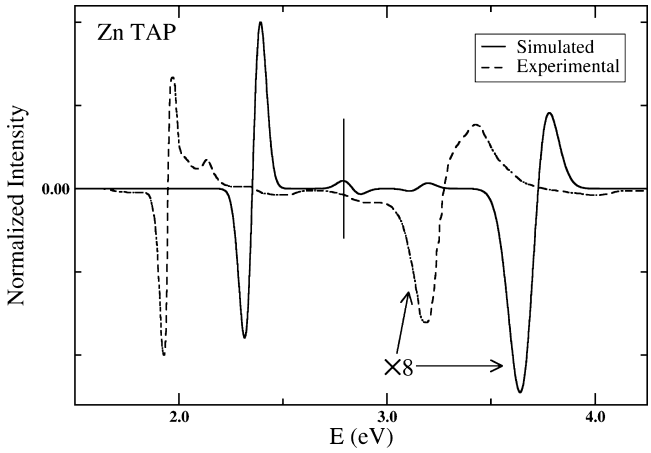

Figure 11. Simulated and experimental[67] MCD of ZnTAP including both *A* and *B* terms in the simulation. The experimental spectrum corresponds to ZnTAPOP with phenyls rather than with hydrogens (ZnTAP) in the b-positions.

is lowest in energy as it does not suffer the same destabilization from N_π orbitals as d_{yz} and d_{xz} . We indicate the d levels

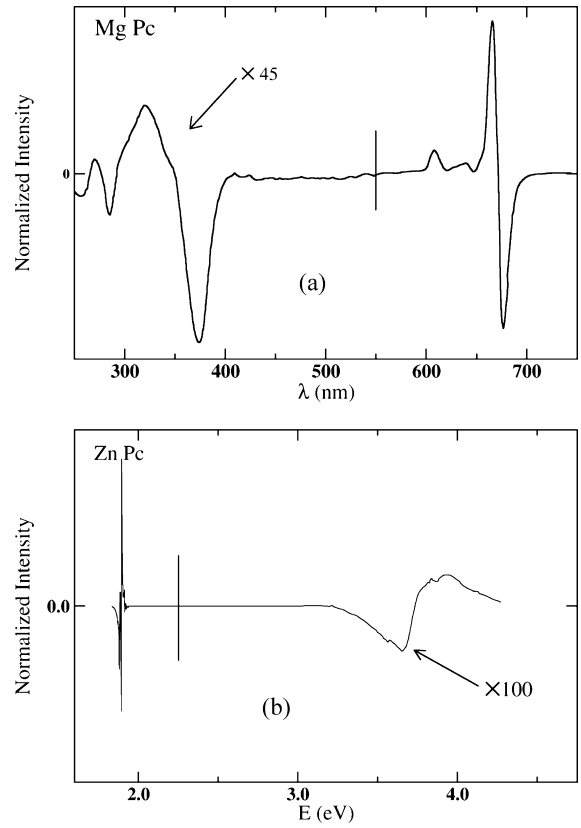

Figure 12. (a) Experimental[68] MCD spectrum for $MgPc(Im)_2$, with Im = imidazole. (b) Experimental[9] MCD spectrum for ZnPc converted to eV.

in Figure 2 in terms of $d_{x^2-y^2}$, d_{z^2}, and so forth, rather than their symmetry labels, b_{1g}, a_{1g}, and so forth. Furthermore, the d levels were not added to the numbering of the levels ($1e_g$, $2e_g$, etc.) to facilitate the comparison between ML systems with different metals (M = Zn, Mg, Ni). The two functions spanning the e_g representation transform as d_{yz} and d_{xz}, respectively. We shall in the following refer to them as e_{gx} and e_{gy}.

3.2. Theoretical and Simulated MCD spectra of MTAP (N = Mg, Ni, Zn). We do not have to consider the *C* term in eq 1 for the tetraazaporphyrin metal complexes investigated here because all of the complexes have a nondegenerate A_{1g} ground state. By contrast, the relatively high symmetry of the MTAP complexes gives rise to *A* terms in the MCD spectra due to the $A_{1g} \rightarrow E_u$ transitions, and we shall in the following give a detailed discussion of the *A* terms for tetraazaporphyrins. *B* terms, that are always possible, will also be discussed. Of the tetraazaporphyrin metal systems studied here, the only published MCD spectrum[67] is for a derivative of ZnTAP with eight phenyl groups in the β positions, which we shall refer to as ZnTAPOP, where the β positions are indicated for MP in Figure 1. Theoretical calculations have previously been carried out on the UV spectra of NiTAP[64] and ZnTAP.[67] However, direct calculations of *A* and *B* term parameters have not previously been published for the MTAP systems.

A general expression for the *A*/*D* parameters for these systems is readily obtained,[19]

$$\frac{A}{D} = -Im\langle\Psi(nE_{ux})|\hat{L}_z|\Psi(nE_{uy})\rangle \quad (4)$$

where nE_{ux} and nE_{uy} are the excited states involved in the *Q*- and Soret-band transitions.

The wave functions for the excited states nE_u responsible for the *Q* or Soret band can for qualitative arguments be expressed as linear combinations of Slater determinants representing the different one-electron excitations involved in the $A_{1g} \rightarrow nE_u$ transition as:

$$\Psi(nE_{ux}) = c_{n1}\left(\frac{1}{\sqrt{2}}|1a_{1u}^{+}2e_{gx}^{-}| - \frac{1}{\sqrt{2}}|1a_{1u}^{-}2e_{gx}^{+}|\right) + c_{n2}\left(\frac{1}{\sqrt{2}}|2a_{2u}^{+}2e_{gy}^{-}| - \frac{1}{\sqrt{2}}|2a_{2u}^{-}2e_{gy}^{+}|\right) + c_{n3}\left(\frac{1}{\sqrt{2}}|1b_{2u}^{+}2e_{gy}^{-}| - \frac{1}{\sqrt{2}}|1b_{2u}^{-}2e_{gy}^{+}|\right) + c_{n4}\left(\frac{1}{\sqrt{2}}|1a_{2u}^{+}2e_{gy}^{-}| - \frac{1}{\sqrt{2}}|1a_{2u}^{-}2e_{gy}^{+}|\right) \quad (5)$$

$$\Psi(nE_{uy}) = c_{n1}\left(\frac{1}{\sqrt{2}}|1a_{1u}^{+}2e_{gy}^{-}| - \frac{1}{\sqrt{2}}|1a_{1u}^{-}2e_{gy}^{+}|\right) - c_{n2}\left(\frac{1}{\sqrt{2}}|2a_{2u}^{+}2e_{gx}^{-}| - \frac{1}{\sqrt{2}}|2a_{2u}^{-}2e_{gx}^{+}|\right) + c_{n3}\left(\frac{1}{\sqrt{2}}|1b_{2u}^{+}2e_{gx}^{-}| - \frac{1}{\sqrt{2}}|1b_{2u}^{-}2e_{gx}^{+}|\right) - c_{n4}\left(\frac{1}{\sqrt{2}}|1a_{2u}^{+}2e_{gx}^{-}| - \frac{1}{\sqrt{2}}|1a_{2u}^{-}2e_{gx}^{+}|\right) \quad (6)$$

Here, c_{ni} is the amplitude by which one-electron excitation number *i* contributes to excited state *n*. The amplitudes can be obtained from the TD-DFT calculations.[2a] The expressions in eqs 5 and 6 reflect the fact that the contributing one-electron excitations are $1a_{1u} \rightarrow 2e_g$ and $2a_{2u} \rightarrow 2e_g$ as well as $1b_{2u} \rightarrow 2e_g$ and $1a_{2u} \rightarrow 2e_g$ (Table 1 and Figures 2 and 4).

Substituting eqs 5 and 6 into eq 4 affords the general expression 7:

$$\frac{A}{D} = -Im(c_{n1}^2 + c_{n2}^2 - c_{n3}^2 + c_{n4}^2)\langle 2e_{gx}|\hat{l}_z|2e_{gy}\rangle + 2c_{n1}c_{n2}Im\langle 1a_{1u}|\hat{l}_z|2a_{2u}\rangle + 2c_{n1}c_{n4}Im\langle 1a_{1u}|\hat{l}_z|1a_{2u}\rangle = T_1 + T_2 + T_3 \quad (7)$$

A similar analysis of the MCD spectrum of zinc phthalocyanine in terms of eq 7 has previously been given by vanCott et al.[9]

The lowering of the $2a_{2u}$ orbital in aza-porphyrins lifts the near degeneracy between $2a_{2u}$ and $1a_{1u}$ observed in regular porphyrins, Figure 4. Thus, we now have in MTAP a *Q* band that has a 85−75% contribution from the $1a_{1u} \rightarrow 2e_g$ one-electron excitation and a 15−25% contribution from the $2a_{2u} \rightarrow 2e_g$ one-electron excitation (Table 1). In the regular porphyrins with a 50/50 contribution from the two one-electron excitations, the calculated intensity of the *Q* band is low as the two transitions contribute with opposite signs to the oscillatory strength[1] *f*. In TAP, such a cancelation is not possible, and we find an intense *Q* band with $f = 0.25-0.5$ (Table 1). The experimental[67] MCD spectrum for ZnTAP (ZnTAPOP) clearly reveals a positive *A* term in the *Q* band region (Figure 7) in agreement with our findings (Table 1 and Figure 8). The calculated $1A_{1g} \rightarrow 1E_u$ excitation energy seems to be overestimated by about 0.4 eV when compared with the observed position of the *Q* band; this might in part be due to the use of a model ZnTAP rather than ZnTAPOP.

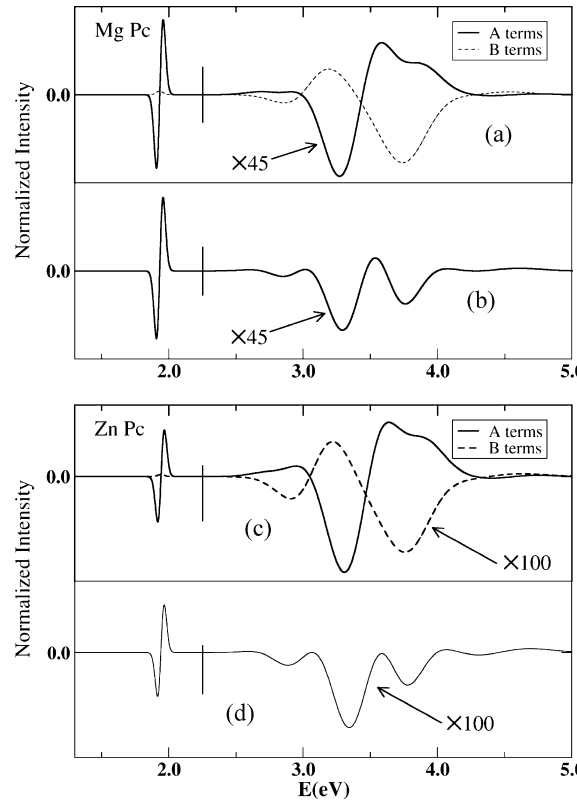

Figure 13. (a) Separate *A* and *B* terms in a simulated MCD spectrum of MgPc. (b) Combined $A + B$ terms in a simulated MCD spectrum of MgPc. (c) Separate *A* and *B* terms in a simulated MCD spectrum of ZrPc. (b) Combined $A + B$ terms in a simulated MCD spectrum.

The positive *A*/*D* term for the *Q* band region is understandable if we make use of eq 7. For MTAP, we have $c_{11} \approx 0.87$, whereas $c_{12} \approx 0.36$, $c_{13} = 0.0$, and $c_{14} = 0.0$. Thus, the first term $T_1 = -(c_{11}^2 + c_{12}^2 - c_{13}^2 + c_{14}^2)\mathrm{Im}\langle 2e_{gx}|\hat{l}_z|2e_{gy}\rangle$ in 7 will contribute with a positive value as in previous ligands[1] since the sign of $Im\langle 2e|\hat{l}_z|2e_{gy}\rangle$ is negative (Table 2). The calculated *A* terms for the *Q* band of the three MTAP systems are very similar with values of 6.86, 6.76, and 7.29 at the calculated excitation energies of 2.32, 2.39, and 2.35 eV for magnesium, nickel, and zinc TAP, respectively (Table 1). These values are much larger than those for the regular porphyrins[1] and reflect the larger intensity gained from lifting the near degeneracy between the $1a_{1u} \rightarrow 2e_g$ and $2a_{2u} \rightarrow 2e_g$ transitions. However, it is interesting that the corresponding calculated *A*/*D* values of 4.94, 4.56, and 4.89 (Table 1) are similar to those found for the regular porphyrins.[1] The three MTAP complexes exhibit in addition a medium-sized positive *B* term (Table 1 and Figure 9) in the *Q*-band region due to the $A_{1g} \rightarrow 1E_u$ transition. The *B* term makes the *A* term in the combined simulated MCD spectrum appear unsymmetrical with the positive lobe larger than the negative lobe (Figure 10). However, the experimental MCD spectrum of ZnTAP seems to reveal that the negative lobe is larger. Unfortunately, a moment analysis of the MCD spectrum for the *Q* band of ZnTAPOP is not available.

For the regular porphyrins, the Soret region is dominated by two transitions due to the $1b_{2u} \rightarrow 2e_g$ one-electron

Table 3. Calculated excitation energies (eV), oscillator strength (f), $A^{b,c}$, A/D, B^b and **B/D** parameters for MPc (M = Mg, Zn)

		exc. energ.									
complex	symmetry	expt	calcd	composition	%	*f*	*A*	*A/D*	*B*	*B/D*	assign.
MgPc	$1E_u$	1.84[a]	1.93	$2a_{1u} \rightarrow 2e_g$	90.87	0.707	20.11	4.04	642.65	129.17	*Q*
	$2E_u$		2.82	$1b_{2u} \rightarrow 2e_g$	97.23	0.034	−0.45	−2.78	−29.99	−183.74	
	$3E_u$		3.01	$2a_{2u} \rightarrow 2e_g$	73.22	0.056	0.55	2.16	−465.41	−1822.87	
				$1a_{2u} \rightarrow 2e_g$	18.5						
				$2b_{1u} \rightarrow 2e_g$	6.35						
				$1b_{1u} \rightarrow 2e_g$	82.08						
	$4E_u$		3.09	$2a_{1u} \rightarrow 3e_g$	7.54	0.202	−1.67	−1.88	607.57	683.80	
	$1A_{2u}$		3.27	$1e_u \rightarrow 2e_g$	99.36	0.001	0.00	0.00	7.55	1722.89	
	$5E_u$		3.30	$2a_{1u} \rightarrow 3e_g$	84.45	0.011	−0.03	−0.64	195.32	4145.54	
				$1b_{1u} \rightarrow 2e_g$	5.41						
				$1a_{1u} \rightarrow 2e_g$	53.04						
	$6E_u$	3.40[c]	3.42	$1a_{2u} \rightarrow 2e_g$	25.76	0.932	10.09	2.72	−149.18	−40.24	B_1
				$2a_{2u} \rightarrow 2e_g$	6.5						
	$7E_u$	3.65[c]	3.74	$1a_{1u} \rightarrow 2e_g$	53.04	1.136	3.47	0.84	−926.15	−223.99	B_2
				$1a_{2u} \rightarrow 2e_g$	25.76						
ZnPc	$1E_u$	1.89[d]	1.94	$2a_{1u} \rightarrow 2e_g$	91.69	0.714	19.89	3.98	629.08	125.74	*Q*
	$2E_u$		2.84	$2b_{2u} \rightarrow 2e_g$	97.14	0.030	−0.40	−2.78	−46.42	−322.71	
				$2a_{2u} \rightarrow 2e_g$	68.82						
	$3E_u$		3.04	$1a_{2u} \rightarrow 2e_g$	14.23	0.062	0.46	1.68	−902.26	−3269.29	
				$1b_{1u} \rightarrow 2e_g$	13.68						
				$1b_{1u} \rightarrow 2e_g$	76.01						
	$4E_u$		3.11	$2a_{2u} \rightarrow 2e_g$	10.43	0.310	−2.09	−1.54	966.95	711.80	
				$2a_{1u} \rightarrow 3e_g$	5.77						
				$1a_{2u} \rightarrow 2e_g$	4.38						
	$5E_u$		3.32	$2a_{1u} \rightarrow 3e_g$	88.42	0.036	−0.11	−0.76	160.79	1095.47	
				$1b_{1u} \rightarrow 2e_g$	5.13						
	$1A_{2u}$		3.34	$1e_u \rightarrow 2e_g$	99.14	0.001	0.00	0.00	15.74	3891.43	
				$1a_{1u} \rightarrow 2e_g$	46.39						
	$6E_u$	3.41[e]	3.46	$1a_{2u} \rightarrow 2e_g$	39.99	0.640	7.92	3.15	−213.52	−84.87	B_1
				$2a_{2u} \rightarrow 2e_g$	7.51						
				$1a_{1u} \rightarrow 2e_g$	46.97						
	$7E_u$	3.69[e]	3.76	$1a_{2u} \rightarrow 2e_g$	31.18	1.069	3.00	0.78	−721.41	−186.73	B_2
				$2a_{2u} \rightarrow 2e_g$	7.19						

[a] Experimental values due to $Mg(Im)_2$ from ref 68. Here, Im = imidazol. [b] All MCD parameters are in atomic units. [c] From deconvolution of the MCD spectrum corresponding to $Mg(Im)_2$ in the Soret region (ref 68). [d] Ref 9. [e] From deconvolution of the MCD spectrum corresponding to Zn(Im) in the Soret region (ref 69).

excitation and the conjugated Gouterman band ($1a_{1u} \rightarrow 2e_g$ and $2a_{2u} \rightarrow 2e_g$), respectively[1]. Further, the transition represented by $1b_{2u} \rightarrow 2e_g$ gains some intensity by mixing with the Gouterman band. The simulated MCD spectrum is dominated by a pseudo-*A* term made up of two *B* terms of opposite sign from each of the transitions.[1]

The Soret region for the aza systems MgTAP and ZnTAP, which we shall discuss next, is dominated by the three one-electron excitations $1b_{2u} \rightarrow 2e_g$, $2a_{2u} \rightarrow 2e_g$ and $1a_{2u} \rightarrow 2e_g$ (Table 1). The $1b_{2u} \rightarrow 2e_g$ excitation gives rise to the very weak $A_{1g} \rightarrow 2E_u$ transition with a calculated absorption energy of 2.8 eV. The transition has a small negative *A* term (Table 1 and Figure 8) and a positive *B* term (Figure 9). In the complete MCD simulation where *A* and *B* terms are combined, $2E_u$ exhibits a positive *B* term at 2.8 eV for both MgTAP and ZnTAP (Figure 10).

The $2a_{2u} \rightarrow 2e_g$ and $1a_{2u} \rightarrow 2e_g$ excitations couple into the $A_{1g} \rightarrow 3E_u$ and $A_{1g} \rightarrow 4E_u$ transitions of which the first calculated at 3.08 to 3.16 eV is weak (f = 0.1 to 0.16), whereas the second at 3.7 eV is strong (f = 3.28 to 1.15), as shown in Table 1. The excited state $3E_u$ exhibits for M = Mg, Zn small positive *A* and *B* terms with A = 0.55 (Mg) and 0.18 (Zn) at 3.08 eV (Mg) and 3.16. eV (Zn) (Table 1 and Figures 7 and 8). The $4E_u$ state is represented by a relatively strong positive *A* term (1.33−1.55), as shown in Figure 8, and a negative *B* term, as shown in Figure 9. In the combined MCD simulation, $4E_u$ appears with a positive *A* term made asymmetric by a negative *B* term (Figure 10), in good agreement with experiment for ZnTAP (Figure 11). It is also in agreement with the experiment that the simulated MCD spectrum in the *Q* region with one positive *A* term has a larger term parameter than the positive *A* term in the Soret region (Figure 11). The calculated excitation energy in the Soret region of ZnTAP corresponding to the $A_{1g} \rightarrow 4E_u$ transition seems to be overestimated just as it was the case for the $A_{1g} \rightarrow 2E_u$ transition in the *Q* band by 0.4 eV. However, the main features of the MCD spectrum for ZnTAPOP are well represented in the simulated spectrum for ZnTAP, both in the *Q* and Soret regions (Figure 11).

The calculated spectrum for NiTAP in the Soret region is more complicated than those for MgTAP and ZnTAP due to the additional participation of the $1e_u \rightarrow 1b_{1g}$ and the $1e_g \rightarrow 1b_{1u}$ one-electron excitations. The new orbitals introduced are shown in Figure 5. In the simulated MCD spectrum of NiTAP, we note for the Soret region that $2E_u$ ($1b_{2u} \rightarrow 2e_{1g}$) appear as a weak negative *A* term as for MgTAP and ZnTAP (Figure 8). We have in addition for the $A_{1g} \rightarrow 4E_u$ ($1e_g \rightarrow 1b_{1u}$, $2a_{2u} \rightarrow 2e_g$) and $A_{1g} \rightarrow 5E_u$ ($1e_u \rightarrow 1b_{1g}$, $1e_g \rightarrow 1b_{1u}$) transitions with medium strong *B* terms (Table 1 and Figures 8 and 9). Unfortunately, to date no experimental MCD spectrum of NiTAP has been published for comparison.

4.2. The MCD Spectra of the Phthalocyanine Complexes MgPc and ZnPc. The phthalocyanine ligand (*Pc*) differs from the simple porphyrin (P) (Figure 1) in having

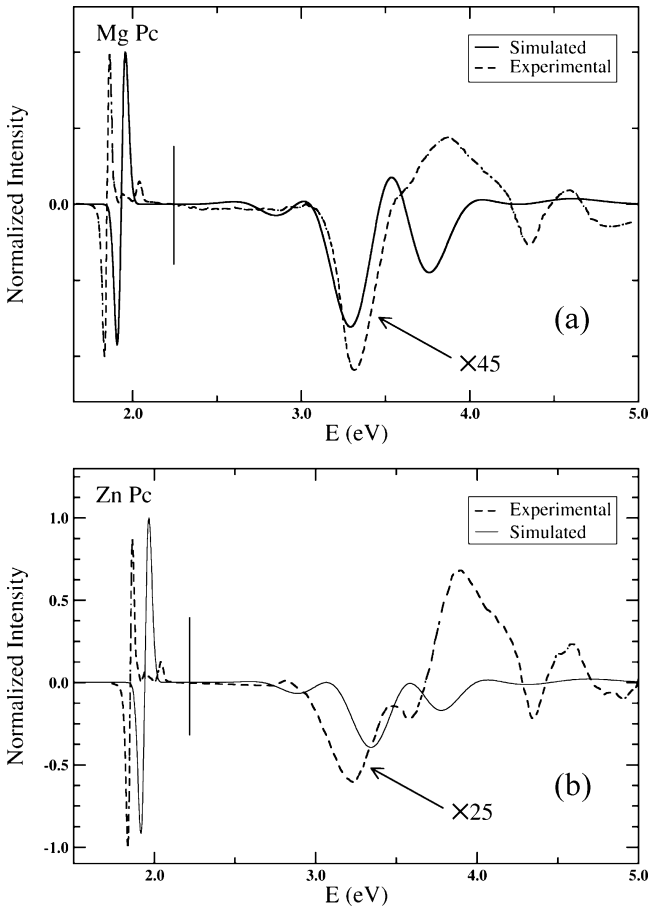

Figure 14. (a) Experimental[68] MCD spectrum of $MgPc(Im)_2$ compared to a simulated spectrum of MgPc based on both *A* and *B* terms. (b) Experimental[69] MCD spectrum of ZnPc(Im) compared to simulated spectrum of ZnPc based on both *A* and *B* terms.

substantial substitutions in both the *m* and the β positions. We have already seen from the porphyrazine complexes MTAP that an aza substitution in the *m* positions gives rise[30] to a lowering in energy of the $2a_{2u}$ orbital (Figure 4). This orbital is in the MP systems, nearly degenerate with the $1a_{1u}$ orbital (Figure 4). The result of the $2a_{2u}$ stabilization is that the *Q* band in the MTAP systems mostly was made up of $1a_{1u} \rightarrow 2e_g$ transition (Table 1), whereas it is a 50:50 mixture of $1a_{1u} \rightarrow 2e_g$ and $2a_{2u} \rightarrow 2e_g$ for MP[1]. On the other hand, the Soret band, which in MP is dominated by two transitions, namely the conjugated Gouterman band (50:50 $1a_{1u} \rightarrow 2e_g$ and $2a_{2u} \rightarrow 2e_g$) and the $1b_{2u} \rightarrow 2e_g$ transition, is in the MTAP systems (M = Mg, Zn), dominated in terms of intensity by three transitions. One transition is made up of the $1b_{2u} \rightarrow 2e_g$ one-electron excitation, and the two other transitions consist of mixtures of the $2a_{2u} \rightarrow 2e_g$, $1a_{1u} \rightarrow 2e_g$, and $1a_{2u} \rightarrow 2e_g$ one-electron excitations.

Apart from the aza substitution in the *m* position, MPc also has the addition of a butadiene unit on each of the four pairs of adjacent β carbons to form four fused benzene rings (Figure 1). The fused rings give rise to a number of new π orbitals[30] representing the upper occupied and lower unoccupied valence levels (Figure 3). Of these orbitals, $3e_g$ is empty and made up of π^*_{Bz} on the different rings (Figure 6), whereas the occupied levels $1b_{1u}$, $1a_{1u}$, $1b_{2u}$, and $2a_{2u}$ are represented by the benzene HOMO orbitals π_{Bz} (Figures 3 and 6). In addition, $2e_g$ and $2a_{1u}$ are constructed from $2e_g$ and $1a_{1u}$ of MTAP by adding an out-of-phase contribution from the butadiene HOMO orbital π_2.

We shall now turn to an assignment of the experimental MCD spectra for MgPc (part a of Figure 12) and for ZnPc (part b of Figure 12) based on our simulated spectra (Figure 13). Our simulations included both *A* and *B* terms. The *Q* band is exclusively made up of a $2a_{1u} \rightarrow 2e_g$ one-electron excitation, and the transition energies for $A_{1g} \rightarrow 1E_u$ of 1.93 eV (Mg) and 1.94 eV (Zn) are in good agreement with the experimental values of 1.84[68] eV (Mg) and 1.89[9] eV (Zn) (Table 3). Many other[9,64,68,69] experimental and theoretical studies have assigned the $2a_{1u} \rightarrow 2e_g$ one-electron transition to the *Q* band.

We compare in Figure 14 the simulated and experimental MCD spectra. The simulated MCD spectra in the *Q*-band region contain an intense positive *A* term and a positive *B* term (parts a and c of Figure 13) that combined appear as a positive *A* term (parts b and d of Figure 13), in agreement with experiment (Figure 12). The calculated *A*/*D* values of 4.04 for MgPc and 3.98 for ZnPc (Table 4) are in reasonable agreement with the experimental values of 2.68 for $MgPc(Im)_2$[68] and 4.2 for ZnPc.[9] It is not clear whether the ZnPc molecules are ordered in the experimental setting of ref 9. If they are ordered, the experimental estimate must be divided by 2 before a comparison with our theoretical value can be carried out. Nyokong[69] et al. find positive *A*/*D* values as well for the two derivatives ZnPc(Im) (1.51) and $ZnPc(CN)^-$ (3.55) (Table 4). Both theory and experiment find that the *Q* band contains a single positive *B* term for all of the MgPc and ZnPc type system. As for the *A*/*D* values, the theoretical *B*/*D* term parameters are overestimated by a factor of 2−3 compared to experiment. The larger theoretical *A*/*D* and *B*/*D* ratios translate into larger theoretical values for the *A* and *B* term parameters as well (Table 4). We note on the other hand a reasonable agreement between theoretical and experimental *D* values (Table 4).

Our calculations on MgPc and ZnPc predict the existence of a number of transitions of low intensity in the region between 2.80 and 3.35 eV (Table 3). Of these, $1A_{1g} \rightarrow 2E_u$ ($1b_{2u} \rightarrow 2e_g$), $A_{1g} \rightarrow 3E_u$ ($2a_{2u} \rightarrow 2e_g$) and $A_{1g} \rightarrow 4E_u$ ($1b_{1u} \rightarrow 2e_g$) are similar in energy and composition. They consist of excitations from π_{Bz} orbitals to $2e_g$. Another involves the excitation from the HOMO $2a_{1u}$ to the π^*_{Bz}-ring combination ($3e_{g1}$). The transitions $A_{1g} \rightarrow nE_u$ (n = 2,5) are weak and situated at the onset of the broadband observed[68,9] with a maximum around 3.5 eV. It is thus not likely that they can be observed (distinguished) individually.

We find for both MgPc and ZnPc that the Soret band in terms of intensity is dominated by the two one-electron excitations $1a_{1u} \rightarrow 2e_g$ and $1a_{2u} \rightarrow 2e_g$ and two transitions. The first transition $A_{1g} \rightarrow 6E_u$ is calculated at 3.42 eV (Mg) and 3.46

(67) Miwa, H.; Ishii, K.; Kobayashi, N *Chem.—Eur. J.* **2004**, *10*, 4422–4435.
(68) Ough, E.; Nyokong, T.; Creber, K. A. M.; Stillman, M. J. *Inorg. Chem.* **1988**, *27*, 2724–2732.
(69) Nyokong, T.; Gazyna, Z.; Stillman, M. J. *Inorg. Chem.* **1987**, *26*, 1087.

Table 4. Calculated and Observed MCD Parameters[b] for *Q* band of MgPc and ZnPc Complexes

	transition energy (ev)		*A*		*A/D*		*B*		*B/D*		*D*	
compound	expt	calcd	expt	calcd	expt	calcd	expt	calcd	expt	calcd	expt	calcd
MgPc		1.93[a]		20.1[a]		4.04[a]		643[a]		129[a]		4.98[a]
$MgPc(Im)_2$	1.88[c]		9.35		2.54		296		80.6		3.68	
ZnPc	1.89[d]	1.94[a]		19.9[a]	4.2	3.98[a]		629[a]		126[a]		5.01[a]
ZnPc(Im)	1.90[e]		5.55		1.51		225		61.1		3.68	
$ZnPc(CN)^-$	1.89[e]		19.9		3.55		62.9		11.2		5.63	

[a] This work. [b] All MCD parameters are in a.u. [c] Ref 68. [d] Ref 9. [e] Ref 69.

Table 5. Calculated and Observed MCD Parameters[b] for Soret-Band of MgPc and ZnPc Complexes

		transition energy (ev)		*A*		*A/D*		*B*		*B/D*		*D*	
compound	band	expt	calcd	expt	calcd	expt	calcd	expt	calcd	expt	calcd	expt	calcd
MgPc	B1		3.42[a]		10.1[a]		2.72[a]		−149[a]		−40.2[a]		3.71[a]
	B2		3.74[a]		3.47[a]		0.84[a]		−926[a]		−224[a]		4.13[a]
$MgPc(Im)_2$[c]	B1	3.40		2.72		1.27		−207		−133		1.56	
	B2	3.65		0.84		0.57		−60.5		−25.1		2.41	
ZnPc	B1		3.46[a]		7.92[a]		3.15[a]		−213[a]		−84.8[a]		2.51[a]
	B2		3.76[a]		3.00[a]		0.78[a]		−721[a]		−187[a]		3.85[a]
ZnPc[d]	B1	3.71				3.7				−526			
	B2	3.74				4.3				−25.2			
ZnPc(Im)[e]	B1	3.41		3.22		1.60		−43.8		−21.8		2.01	
	B2	3.69		2.53		1.19		−146		−68.9		2.12	
$ZnPc(CN)^-$[e]	B1	3.21		1.81		1.21		−339		−226		1.50	
	B2	3.75		1.87		0.78		−54		−22.5		2.40	

[a] This work. [b] All of the MCD parameters are in a.u. [c] Ref 68, from convolution of the MCD spectrum. [d] Ref 9. [e] Ref 69, from convolution of the MCD spectrum.

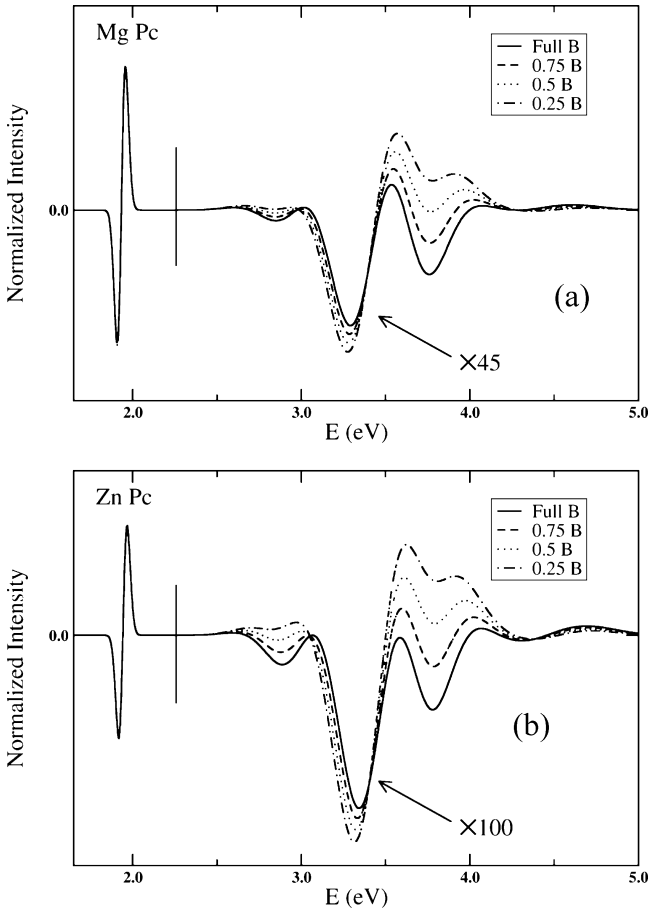

Figure 15. (a) Simulated MCD spectra of MgPc with reduced *B* term. (b) Simulated MCD spectra of ZnPc with reduced *B* term.

eV (Zn), respectively, whereas the second ($A_{1g} \rightarrow 7E_u$) is predicted at 3.65 eV for MgPc and 3.70 eV for ZnPc, respectively (Table 5). We note further that both the $A_{1g} \rightarrow 6E_u$ and the $A_{1g} \rightarrow 7E_u$ transition have a large oscillator strength with an intensity ratio of 6:10. We assign both of these transitions to the broad Soret band observed around 3.5 eV for the two compounds.

We find in agreement with all of the available experimental findings on MPc (M = Mg, Zn) type systems[9,68,69] that the MCD spectra in the Soret region are dominated by two transitions ($A_{1g} \rightarrow 6E_u$ and the $A_{1g} \rightarrow 7E_u$) with positive *A*/*D*-term values and negative *B*/*D*-term values. Our calculated excitation energies are in addition in good agreement with the values deduced by Stillman et al., especially for $MgPc(Im)_2$[68] and ZnPc(Im)[69] (Table 5). A detailed comparison between experiment and theory is hampered by the fact that most of the experiments are on derivatives of MPc. Also, the MCD parameters are obtained by a convolution (fitting) of the MCD spectra in the Soret region. Nevertheless the *A*/*D*-term values seem to compare with experiment within a factor of 2. Assessment of the calculated *B*/*D* terms are made difficult by the fact that Stillman[68,69] et al. in their convolution make use of several *B* terms with different energy centers in the Soret region, whereas we only make use of two.

It follows from parts a and c of Figure 13 that the two positive *A* terms overlap and coalesce into one single positive *A* term with a shoulder on the high-energy positive portion. The two negative *B* terms are also seen in parts a and c of Figure 13 to merge. The result is a single negative *B* term. The sum of the *A* and *B* terms clearly depends on the relative size of their parameters. For the case at hand, we see that the low energy part is dominated by the positive *A* terms and the high energy part by the negative *B* terms (parts b and d of Figure 13. When comparing our simulated MCD spectra for MPc (M = Mg, Zn) in the Soret region with experiment, we note a good agreement at the low-energy

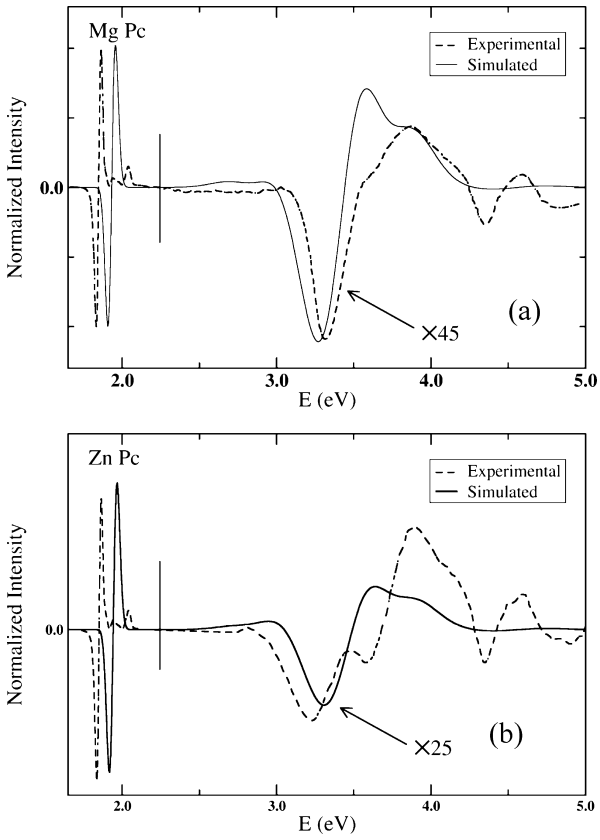

Figure 16. (a) Experimental[68] MCD spectrum of $MgPc(Im)_2$ compared to a simulated spectrum of MgPc based on the *A* term alone. (a) Experimental[69] MCD spectra of ZnPc(Im) compared to a simulated spectrum of ZnPc based on the *A* term alone.

side, whereas the high-energy parts differ considerably (parts a and b of Figure 14. That is, the simulated high-energy part should be positive rather than negative. A possible explanation for this deviation is that the calculated *B* term parameters in absolute terms are too large compared to the calculated *A* term parameters. To explore this possibility, we display in Figure 15 simulated MCD spectra in which the negative *B* term parameters have been reduced by 25, 50, and 75% in absolute terms. Indeed, the agreement between the experimental and simulated MCD spectrum improves with the reduction. Figure 16 displays the limit in which we compare the experimental MCD spectra with simulated spectra made up of *A* terms alone. The consideration given here lead us to conclude that the signs and position of the *A* and *B* terms calculated here for the Soret band likely are correct. However, in absolute terms the *B* term parameters are likely too large compared to the *A* parameters.

5. Conclusions

We have presented a simulation of magnetic circular dichroism (MCD) spectra[1] for phthalocyanine (M = Mg, Zn) and tetraazaporphyrin (M = Mg, Zn, Ni) metal complexes (Figure 1). The MCD simulation was based on a recent implementation[2] into the Amsterdam Density Functional program[3,4] based on time-dependent density functional theory (TD-DFT).

We have previously found in MP[1] that the two occupied levels of highest energy were nearly degenerate and represented by π^* orbitals of a_{2u} and a_{1u} symmetry in agreement with previous calculations as cited in a recent review[30] (Figure 4). The $2a_{2u}$ orbital of the regular porphyrins (MP, MTPP, and MOEP) has a large contribution from the π orbital of the carbon atom in the *m* position, whereas no such contribution[64] is present in $1a_{1u}$. As the carbon atom in MP now is substituted by the more electronegative nitrogen in MTAP and MPc, the energy of $2a_{2u}$ is lowered compared to $1a_{1u}$ where the composition is unchanged[64] (Figure 4). As pointed out by Baerends[30,64] et al., the change in the relative energies of $1a_{1u}$ and $2a_{2u}$ will make the composition of the excited states in MP, MTPP, MOEP quite different from those in MTAP and MPc.

The *Q*-band region is represented by a single electronic transition made up mostly of the one-electron excitation $2a_{1u} \rightarrow 2e_g$ for both the MTAP (M = Mg, Zn, Ni) and MPc (M = Mg, Zn) systems. This is in contrast to the regular MP complexes, where the two excitations $2a_{1u} \rightarrow 2e_g$ and $2a_{2u} \rightarrow 2e_g$ are of equal importance. The MCD spectrum in the *Q*-band region was predicted to contain a single positive *A* term augmented by a single positive *B* term, in agreement with the available experimental[30] data and previous theoretical considerations[24b] (Table 4). The calculated *A*/*D* and *B*/*D* term parameters as well as the dipole strength *D* in the *Q*-band region were in good agreement with experiment. The theoretical parameters are in general on the high side in absolute terms and overestimated in some cases by a factor of up to 2. Whereas the *A*/*D* parameters for MTAP (M = Mg, Zn, Ni) and MPc (M = Mg, Zn) are quite similar to those of the MP complexes in the *Q* region, the MTAP and MPc compounds have larger *A*-term parameters. This is because the two one-electron excitations responsible for the *Q* band in the MP systems interfere destructively to afford a modest dipole strength *D*. This is not possible for the MTAP and MPc compounds, where a single one-electron excitation is involved. In the MP complexes, vibronic coupling gives rise to two *A* terms of similar intensity from the same electronic transition. This doubling is not visible to the same extend for the title compounds. However, it is possible that a dark state seen in some of the title compounds[24] originates from vibronic coupling. Unfortunately, we are not currently able to simulate vibronic coupling effects.

For the aza systems MgTAP and ZnTAP, the MCD spectra in the Soret region are dominated by the two one-electron excitations $2a_{2u} \rightarrow 2e_g$ and $1a_{2u} \rightarrow 2e_g$ (Table 1). The $2a_{2u} \rightarrow 2e_g$ and $1a_{2u} \rightarrow 2e_g$ excitations couple into the $A_{1g} \rightarrow 3E_u$ and $A_{1g} \rightarrow 4E_u$ transitions. The excited state $3E_u$ exhibits for M = Mg, Zn small positive *A* and *B* terms (Table 1 and Figures 9 and 10). The $4E_u$ state is represented by a relatively strong positive *A* term (1.33−1.55), as shown in Figure 8, and a negative *B* term, as shown in Figure 9. In the combined MCD simulation, $4E_u$ appears with a positive *A* term made asymmetric by a negative *B* term (Figure 9), in good agreement with experiment for ZnTAPOP (Figure 11).

We find in agreement with all available experimental findings on MPc (M = Mg, Zn) type systems[9,68,69] that the MCD spectra in the Soret region are dominated by two

transitions ($A_{1g} \rightarrow 6E_u$ and the $A_{1g} \rightarrow 7E_u$) with positive *A*/*D*-term values and negative *B*/*D*-term values. The major contribution to the two transitions come from the $2a_{2u} \rightarrow 2e_g$ and $1a_{2u} \rightarrow 2e_g$ one-electron excitations. Our calculated excitation energies are in addition in good agreement with the values deduced by Stillman et al., especially for MgPc(Im)$_2$[68] and ZnPc(Im)[69] (Table 5). It appears that the ratio *A*/*B* for the term parameters is underestimated by theory in the Soret region. The origin of the MCD spectra in the Soret region for the title compounds is quite different from that of the MP complexes, where two closely spaced *B* terms with the appearance of a single *A* term dominate the Soret region[1].

Acknowledgement. We would like to thank NSERC and the Canada Research Chair program for support of this work.

IC7022117